A. Bergstrand, *J. Cell. Biol.* **32**, 415 (1967).
19. H. Maeno, E. M. Johnson, P. Greengard, *J. Biol. Chem.* **246**, 134 (1971).
20. E. L. Gottfried, *J. Lipid Res.* **8**, 321 (1967).
21. J. P. Williams and P. A. Merrilees, *Lipids* **5**, 367 (1970).
22. J. G. Heider and R. L. Boyett, *J. Lipid Res.* **19**, 514 (1978).
23. C. G. Duck-Chong, *Lipids* **14**, 492 (1979).
24. *Sigma Technical Bulletin* **405**, 1 (1977).
25. We thank I. Ramshaw, B. Sordat, and C. Van Haaften-Day for supplying the cell lines and their many helpful discussions and M. H. N. Tattersall for continued support.

4 June 1984; accepted 29 October 1984

Contribution of Small Glaciers to Global Sea Level

Abstract. *Observed long-term changes in glacier volume and hydrometeorological mass balance models yield data on the transfer of water from glaciers, excluding those in Greenland and Antarctica, to the oceans. The average observed volume change for the period 1900 to 1961 is scaled to a global average by use of the seasonal amplitude of the mass balance. These data are used to calibrate the models to estimate the changing contribution of glaciers to sea level for the period 1884 to 1975. Although the error band is large, these glaciers appear to account for a third to half of observed rise in sea level, approximately that fraction not explained by thermal expansion of the ocean.*

Sea level appears to have risen 10 to 15 cm in the last 100 years, and part of this rise may be due to thermal expansion of the oceans (*1–3*). The remainder has generally been attributed to melting of polar ice. However, studies of the current mass balance of the Antarctic ice sheet, which makes up about 85 percent of the total glacier ice area on the earth, suggest that a negative mass balance is not likely and that this ice sheet may be subtracting water from the world ocean (*4, 5*). Recent estimates of the mass balance of the Greenland ice sheet (12 percent of the world's glacier ice area) suggest that it is close to balance (*4, 6*). If the remaining 3 percent of the earth's glacier ice area accounts for the unexplained rise in sea level, might a further addition to sea level be expected from these small glaciers as the climate warms because of the increased concentration of CO_2 and other "greenhouse" gases?

Because data on glacier measurements are sparse, a 61-year average change in glacier mass was calculated from the meager volume change data and scaled to a global estimate by considering the intensity of the seasonal mass balance fluxes. This result, together with data from the few long-term balance models, is used to estimate the annual contribution of water to the ocean between 1884 and 1975. The Antarctic and Greenland ice sheets and the smaller glaciers near them are not considered.

Glacier observations that are available include measurements of advance or retreat, mass balance histories derived from snow pits and ice cores, volume changes, direct measurements of annual and seasonal mass balances, and mass balance sequences extended by use of numerical models. Most of the data and the longest records are of the first two types and are virtually impossible to use to infer long-term changes in ice mass. Advance-retreat data do not provide volume change information and can be misleading in sign; a glacier can increase in volume and retreat at the same time. Stratigraphic measurements of balances in pits and cores are taken at single locations in the accumulation area, which is insufficient to infer the mass change of the entire glacier. Direct measurements of mass balance, made on the glacier surface, provide short-term results; the oldest series was started in 1945, and only 37 glaciers were being so measured before the beginning of the International Hydrological Decade in 1965. Thus, this analysis is based mainly on long-term volume change data and the results of numerical mass balance models.

The mass balance (b) of a glacier is the difference in water equivalent between input (accumulation) and outgo (ablation) at the surface, averaged over the area of the glacier (G), which is a function of time (t) (*7*)

$$\Delta V = \frac{1}{\rho} \int_{t_0}^{t_1} b(t)G(t)dt \qquad (1)$$

where ΔV is the long-term volume change, and ρ is the specific gravity of the glacier, which is assumed not to change. Because sufficient data are generally not available, I use the approximation

$$\bar{b} = \frac{\rho \Delta V}{(t_1 - t_0)\overline{\overline{G}}} \qquad (2)$$

where $\overline{\overline{G}}$ is the average area of the glacier during the interval $t_0 < t < t_1$, to estimate the long-term mean balance $\bar{b}$ (*8*).

Simple statistical models have been used to develop long-term balance sequences from a short sequence of measured balances combined with long-term records at meteorological and hydrological stations. These hydrometeorological (HM) models generally relate accumulation on the glacier to winter precipitation, ablation to summer air temperature, and the net balance to the difference between accumulation and ablation; runoff may be used to calibrate input and output (*9*). These statistical relations, however, may not be stationary over long periods of time, and as a result the long-term mean balance may be seriously in error (*10*). In very few cases, the estimated mean balances have been calibrated or checked against known volume changes; these calibrated HM models provide results that can be used with confidence (*11*).

Data on glacier balance and volume change for periods exceeding 50 years for 25 glaciers (Table 1) were taken from reports of the Permanent Service on the Fluctuations of Glaciers (*12*) and other sources (*13*). The mean period of record for those glaciers is from 1900.5 to 1961.7; HM sequences for the interval 1900 to 1961 were used to make the data set more homogenous. The unweighted average of the 25 mean balances is -0.40 m/year in water equivalent (standard deviation, 0.25); the mean of the 13 regional averages is -0.34 ± 0.20 m/year; and the mean of the regional averages weighted by quality of the data (*14*) is -0.38 ± 0.20 m/year.

The 25 glaciers with long-term data occur in only 13 regions (Table 1) and constitute a biased sample of the world's glaciers: all but one are between 38° and 69°N latitude; none is at low latitudes or in the Southern Hemisphere. Thus a method is needed to relate these results to an estimate of the mass balance of the earth's entire cover of glaciers.

I suggest that the magnitude of the long-term balance may be related to the magnitude of the seasonal mass fluxes (accumulation and ablation) and that this may be used as a scaling factor to derive global estimates. The annual mass balance amplitude is defined as

$$a = (b_w - b_s)/2 \qquad (3)$$

where b_w is the winter balance and b_s (normally negative) is the summer balance (*7, 15*). Winter and summer balances are used instead of annual accumulation and ablation, respectively, which are rarely measured. Values of the annual amplitude can be calculated for most of the world's glacier areas from data reported since 1965 (*12*) and can be estimated for other areas because annual amplitude is primarily a function of the climatological regime. The annual amplitude is highest at temperate to subarctic (and subantarctic) latitudes, lowest near the poles, and also decreases with increasing continentality (Table 1). Gla-

ciers in the polar regions, large in aggregate area, are not thinning and receding as rapidly as those in more temperate latitudes (*16*), but few long-term data are available.

The 1900 to 1961 data (Table 1) are averaged by region and then scaled to a global average in terms of sea level change by

$$h(1961) - h(1900) = -\frac{1}{J}\left[\sum_{j=1}^{J}\frac{\bar{b}_j}{a_j}\right] \times \left[\sum_{k=1}^{K}(a_k\bar{G}_k)\right]A^{-1} \quad (4)$$

where h is the sea level equivalent of global glacier balance (without consideration of elastic, plastic, or thermal compensation of the ocean or the earth), $\bar{b}_j$ is the average balance change in the j-th region for the period 1900 to 1961 (J = 13, Table 1), a_j is the annual amplitude associated with the $\bar{b}_j$, $\bar{G}_k$ is the 1900 to 1961 average of the area of glacial ice in the k-th region of the world (K = 31, Table 1), a_k is the average annual amplitude associated with each $\bar{G}_k$, and A is the area of the world's ocean (*17*).

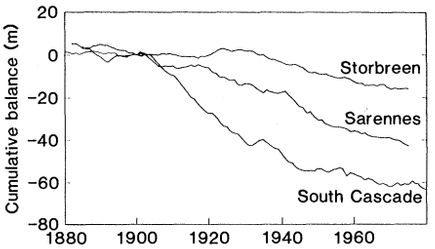

Fig. 1. Cumulative mass balance of water equivalent of Storbreen, South Cascade, and Sarennes glaciers (*9, 22, 23*). All values are relative to 1900.

This scaling procedure assumes a relation between $\bar{b}$ and a. For the 13 regional averages, the correlation coefficient between the two quantities is −0.55 and the average value of the fraction $\bar{b}/a$ is −0.23 (standard deviation, 0.12). Thus, the implied relation is only crudely supported by the data. The $\bar{G}_k$ in Eq. 4 can only be estimated from recent values. Earlier maps are notoriously inaccurate. Because the actual ice area has been shrinking, use of recent values produces an underestimate of the contribution to sea level. Areal shrinkage of the glaciers in the 13 regions where long-term changes were observed ranges from about 5 to 44 percent in 61 years; the average underestimate in the global contribution is estimated at 10 ± 5 percent because in areas of large ice cover (such as arctic Canada and southern Alaska) the shrinkage has been much less than in those areas (for example, the Alps and Scandinavia) where most of the observations have been made. This problem also

Table 1. Long-term balances ($\bar{b}$), annual balance amplitude (a), glacier area (G), amplitude-area product (aG), and location by region for 25 glaciers (*13*). Parentheses indicate values estimated on climatological grounds. Methods for obtaining balances are: A, estimate of long-term volume change; B, measured long-term volume change; C, estimate of long-term volume change for all glaciers in the country; D, uncalibrated HM model; and E, HM model calibrated with long-term volume change. The estimated contribution of each region to global sea level is proportional to aG.

Region	Balance			Amplitude		G (km^2 × 10^3)	aG (km^3/year)	Centroid of area	
	$\bar{b}$ (m/year	Method	N	a (m/year)	N			Latitude	Longitude
Canadian Arctic-North			0	0.28	6	108.6	30.0	79°N	81°W
Baffin and Bylot Islands, Labrador			0	0.40	2	42.0	17.0	70°N	71°W
Brooks Range, Kigluaik Mountains	−0.2	A	1	0.90	1	0.7	.6	68°N	147°W
Alaska Range; Talkeetna, Kilbuk Mountains	−0.55	B	1	1.09	1	14.9	16.0	63°N	151°W
Aleutian Islands, Alaska Peninsula			0	(1.0)	0	2.2	2.2	56°N	159°W
Coastal Mountains Kenai Peninsula to 55°N	−0.4	A	1	2.54	3	88.4	225.0	60°N	140°W
Mackenzie, Selwin, Rocky Mountains north of 55°			0	(1.0)	0	0.9	.9	60°N	128°W
Coast Mountains south of 55°N, Cascades, Olympics	−0.71	B, D, E	3	3.24	6	14.0	45.0	51°N	124°W
Rocky Mountains south of 55°N, Selkirks (Canada), Northern Rocky Mountains	−0.22	B	1	1.30	2	4.0	5.2	52°N	118°W
Middle and Southern Rocky Mountains, Sierra Nevada	−0.34	A, B	2	2.24	4	0.1	.2	43°N	112°W
Mexico			0	(1.0)	0	0.01	.01	19°N	98°W
Andes, 10°N to 0°			0	(1.0)	0	0.05	.05	4°N	77°W
Andes, 0° to 30°S			0	0.98	2	5.2	5.1	13°S	74°W
Andes, 30°S to 55°S			0	(2.5)	0	31.0	77.0	48°S	73°W
South Atlantic Islands			0	(1.0)	0	4.1	4.1	57°S	35°W
Iceland, Jan Mayen	−0.63	C	1	1.88	2	11.3	21.0	65°N	17°W
Svalbard			0	0.88	5	38.8	34.0	79°N	18°E
Franz Josef Island, Novaya Zemlya	−0.13	D	1	0.41	1	37.7	15.0	78°N	59°E
Severnaya Zemlya, other Soviet arctic islands			0	(0.4)	0	18.4	7.4	79°N	98°E
Norway, Sweden	−0.21	B, E	2	2.16	10	3.1	6.7	63°N	11°E
Alps, Pyrenees	−0.42	B, C, E	8	1.28	4	2.9	3.7	46°N	8°E
Caucasus, Turkey, Iran	−0.28	B, D	2	2.36	1	1.5	3.5	43°N	45°E
Ural Mountains, Byrranga, Putorana	−0.35	D	1	2.38	2	0.1	0.2	66°N	61°E
Hindukush, Pamir, Alai, Karakorum, Himalaya, Nyainqentangla			0	1.34	2	76.7	103.0	35°N	76°E
Tien Shan, Kun Lun, Altai, Qilian Shan, Dzungaria, Sayan	−0.02	D	1	.83	8	32.1	27.0	36°N	82°E
Kodar, Orulgan, Chersky, Sun-Kho, Koryasky			0	(0.7)	0	0.6	0.4	63°N	141°E
Kamchatka			0	3.67	1	0.9	3.3	56°N	160°E
Africa			0	0.83	1	0.01	0.01	1°S	35°E
West Irian			0	1.88	1	0.02	0.04	4°S	137°E
New Zealand			0	4.80	2	1.0	4.8	45°S	170°E
Kerguelen, Heard Island			0	1.00	1	0.9	0.9	51°S	71°E
Total			25		68	542.2	661.0		

applies to some of the HM model and volume change results; therefore I raise the calculated values by 10 percent in 61 years.

These scaled results suggest a 61-year rise in sea level of 0.46 ± 0.26 mm/year (*18, 19*). The effect of the assumption about scaling by annual amplitude can be seen by examining two extreme cases: no scaling yields an estimate of global sea level change of 0.57 mm/year; if no change has occurred in high latitudes (>70°), the estimate of sea level change is 0.36 mm/year. Both extreme values lie within the estimated error limits of the scaled result.

Examination of the $a\overline{G}$ products (Table 1) shows that more than a third of the calculated glacier contribution to sea level comes from the mountains bordering the Gulf of Alaska; also, the high mountains of Central Asia and the Patagonian Andes make appreciable contributions. Analysis of these areas (especially the latter) is hampered by a paucity of data.

Year-by-year variations were investigated by use of balance sequences derived from HM models. It has been shown that within a given region, annual balances from different glaciers are highly correlated (*20*). However, annual variations are large compared with long-term trends and are poorly correlated from region to region (*21*). Therefore, a global, long-term combination of balance histories can be treated as a combination of uncorrelated variables.

There are three well-calibrated HM models: South Cascade Glacier, North Cascades, United States (*9*); Storbreen, Norway (*22*); and Sarennes Glacier, France (*23*). Their mean balances for the period 1900 to 1961 are, respectively, −1.13, −0.22, and −0.57 m/year, bracketing the 25-glacier average of −0.40 m/year. For the longest period of simultaneous results (1884–1975), they show balance averages of, respectively, −0.82, −0.17, and −0.41 m/year, but with some nonsynchronous fluctuation (Fig. 1).

The time change in the contribution of these small glaciers to global sea level $h(t)$ can be estimated by

$$h(t) - h(1900) = \frac{h(1961) - h(1900)}{3} \times \sum_{i=1}^{3} [f_i(t)/f_i(1961)] \quad (5)$$

where

$$f_i(t) = \int_{1900}^{t} b_i(t)dt$$

the $b_i(t)$ are balance series from the three calibrated HM models (South Cascade, Stor, and Sarennes Glaciers), and $h(1961) - h(1900) = 28$ mm $= 61$ year $\times$ 0.46 mm/year.

Figure 2 shows the estimated meltwater input to the oceans for $h(t) - h(1900)$ and two recent sea level curves (*2, 3*). Small glaciers appear to account for a third to half of the sea level rise observed since 1884, and the amount of rise is approximately equal to that not explained as thermal expansion by Gornitz *et al.* (*2*). Also, the shapes of the two curves are not completely dissimilar, and the glacier melt curve roughly parallels the variation in global air temperature (*24*). However, these apparent consistencies need to be considered in light of (i) wide error limits including variances in the data of about 60 percent of the total change from 1900 to 1961, (ii) the uncertain assumption that observed values can be scaled to a global mean with mass balance amplitudes, (iii) the further assumption that $h(t)$ is proportional to the average $b(t)$ of three well-studied glaciers, and (iv) the fact that those regions that probably contribute most substantially to sea level rise are underrepresented by observations.

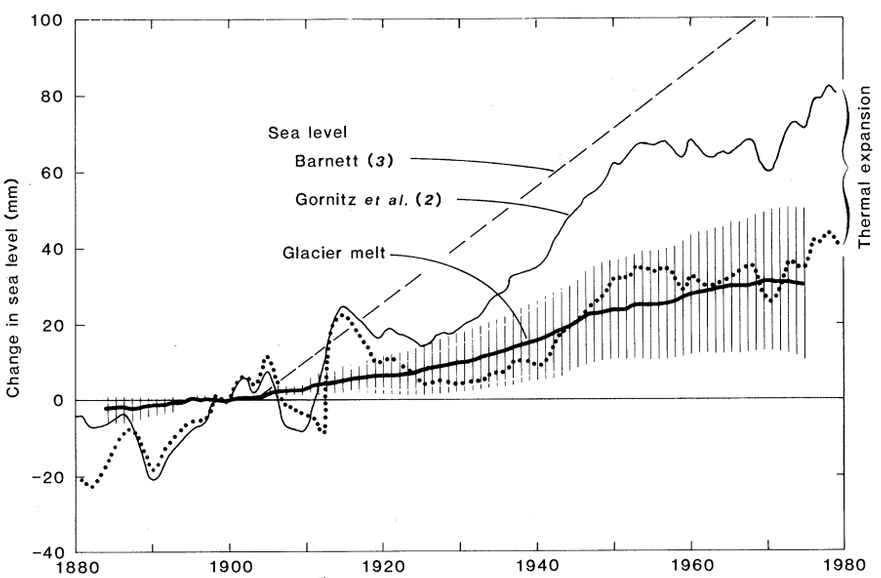

Fig. 2. Contribution of small glaciers to global sea level change (heavy line with vertical lines indicating error limits), together with sea level curves according to Barnett (*3*) and Gornitz *et al.* (*2*). Also shown is an estimate of sea level change due to thermal expansion (*2*) subtracted from the sea level curve of Gornitz *et al.* (dotted line). Thus, the fraction of sea level change below the dotted line is that part not explained as thermal expansion by them. All values are relative to 1900. The thermal expansion curve taken from (*2*) is that for the preferred value of equilibrium sensitivity for doubled CO_2 of 2.8°C.

Although the small glaciers of the world have been decreasing in size over the last 60 to 100 years, there is no direct evidence that this has been caused by an increased concentration of CO_2 and other gases in the atmosphere. The concentration of CO_2 increased appreciably during the period 1960 to 1975 (*25*) at a time when the small glaciers were nearly in balance (*12*) (Fig. 2). Existing HM models provide a means of estimating changes in the melt rate due to long-term changes in atmospheric temperature. Coefficients applied to summer air temperature range from 0.57 m/year per degree Celsius (*22*) to 0.98 m/year per degree Celsius (*9*). A doubling of atmospheric CO_2 concentration might lead to a rise in air temperature of 1.5° to 4.5°C (*26*), which could produce a rate of sea level rise due to small glacier melt of 1.3 to 6.6 mm/year, all other factors being held constant; from the average of the HM coefficients, the 1.5° to 4.5°C range in temperature rise would correspond to a more probable rate of sea level rise of 1.7 to 5.2 mm/year. If the concentration doubled in 100 years and if the rise in the annual meltwater contribution were linear, the probable contribution to sea level rise would be about 0.09 to 0.26 m. Air temperature rose about 0.5°C from 1900 to 1961, and glacial wastage produced a 28-mm rise in sea level; this suggests that sea level will rise 0.08 to 0.25 m in the next 100 years because of ice melt if the air temperature rises 1.5° to 4.5°C. The actual sea level rise might be less because the area of glacier ice will have diminished, and precipitation may increase in many regions, offsetting the wastage. But other meltwater contributions to sea level, such as from the large ablation area of the Greenland ice sheet, may be far more important.

MARK F. MEIER

U.S. Geological Survey
Tacoma, Washington 98402

References and Notes

1. R. Etkins and E. S. Epstein, *Science* **215**, 287 (1982); R. R. Revelle, in *Changing Climate* (National Academy of Sciences, Washington, D.C., 1983), pp. 443–448; A. Robock, *Science* **219**, 996 (1983).
2. V. Gornitz, S. Lebedeff, J. Hansen, *Science* **215**, 1611 (1982).
3. T. P. Barnett, *Clim. Change* **5**, 15 (1983).
4. M. F. Meier, *Hydrol. Sci. J.* **28**, 3 (1983).
5. C. R. Bentley, in *Climate Processes and Climate Sensitivity*, J. E. Hansen and T. Takahashi, Eds. (Maurice Ewing Series 5, American Geophysical Union, Washington, D.C., 1984), pp. 207–220.
6. U. Radok *et al.*, *Climatic and Physical Characteristics of the Greenland Ice Sheet* (Cooperative Institute for Research in Environmental Sciences, Boulder, Colo., 1982); R. A. Bindschadler, *J. Geophys. Res.* **89**, 2066 (1984).
7. International Association of Scientific Hydrology, *Tech. Pap. Hydrol.* 5 (1970); L. R. Mayo *et al.*, *J. Glaciol.* **11**, 3 (1972). The distinction between annual and net balances, important for a given year, becomes unimportant for the long time series discussed here.
8. In some cases G_0 is not given; in others only mean thickness change is given. In these cases only G_1 is known and the resulting $\bar{b}$ is underestimated.
9. W. V. Tangborn, *J. Glaciol.* **25**, 3 (1980).
10. At least one uncalibrated HM model gives a long-term $\bar{b} > 0$ for a glacier that was shrinking.
11. However, the changing glacier area $G(t)$ must be known to translate $b(t)$ to meltwater volume; this is generally not reported, resulting in an underestimate similar to that described in (*8*).
12. International Association of Scientific Hydrology, *Fluctuations of Glaciers* (Unesco, Paris, 1967), vol. 1; *ibid.* (1973), vol. 2; *ibid.* (1977), vol. 3.
13. M. F. Meier, unpublished compendium of data sources.
14. Quality weights used are 4/7 for calibrated HM models and high-quality volume change observations, 2/7 for other volume change observations, and 1/7 for volume change estimates and uncalibrated HM models.
15. In areas of monsoon climate and in some high polar areas, the expression $a = (|b_w| + |b_s|)/2$ was used.
16. R. Koerner (unpublished manuscript) notes that many ice caps and outlet glaciers in arctic Canada show no measurable change in the last several decades; others show thinning, areal shrinkage, or retreat, especially during the period 1950 to 1970. Some small ice caps have disappeared, but the changes are "not especially dramatic."
17. The a_j and a_k in Eq. 4 represent average values during the period 1965 to 1975 (in some cases, even shorter periods), which was a period of extensive measurement. These values are used as estimates of unknown longer term average values $\bar{a}$. Because it seems unlikely that the a_j would have varied as much through time as b_j, the error introduced is probably small.
18. The estimated standard error is the combination of variances in all data sets used in Eq. 4 (±0.25 mm/year), plus an estimate of the error due to sometimes unknown decreases in area (±5 percent).
19. S. Thorarinsson [*Geogr. Ann.* **22**, 131 (1940)] estimated a similar rate of sea level rise due to glacial shrinkage in the 1920's and 1930's.
20. L. Renaud, *Int. Assoc. Sci. Hydrol. Publ. 126* (1980), p. 273.
21. For the period 1965–75, correlation coefficients for the average annual balances between pairs of ten regions range from −0.44 to +0.53. For seven long-term balance series, all in different regions, the correlation coefficients range from −0.48 to +0.45. O. Orheim [*Ohio State Univ. Inst. Polar Stud. Rep. 42* (1972)] notes that using 10-year moving averages greatly improves the correlations.
22. O. Liestøl, *Storbreen Glacier in Jotunheim, Norway* (Norsk Polarinstitutt, Oslo, 1967), p. 141.
23. S. Martin, *Zeit. Gletscherkunde u. Glazialgeologie* **13**, 127 (1978).
24. J. Hansen *et al.*, *Science* **213**, 957 (1981); G. Weller *et al.*, in *Changing Climate* (National Academy of Sciences, Washington, D.C., 1983), pp. 292–382.
25. L. Machta, in *Changing Climate* (National Academy of Sciences, Washington, D.C., 1983), pp. 262–265.
26. Climate Research Board, *Carbon Dioxide and Climate—A Scientific Assessment* (National Academy of Sciences, Washington, D.C., 1979); *Carbon Dioxide and Climate—A Second Assessment* (National Academy of Sciences, Washington, D.C., 1982).

27. I thank S. Ommaney, R. Koerner, V. Kotliakov, and P. Holmlund for access to unpublished material, Cao Meisheng for help in translation of Chinese sources, B. Vaughn and D. Smith for assisting in data compilation, L. A. Rasmussen for much helpful discussion, J. Hansen, L. A. Rasmussen, and C. R. Bentley for useful manuscript reviews, an anonymous reviewer for locating a numerical error, and T. P. Barnett who suggested that I look into this question.

19 April 1984; accepted 25 July 1984

A Circumstellar Disk Around β Pictoris

Abstract. *A circumstellar disk has been observed optically around the fourth-magnitude star β Pictoris. First detected in the infrared by the Infrared Astronomy Satellite last year, the disk is seen to extend to more than 400 astronomical units from the star, or more than twice the distance measured in the infrared by the Infrared Astronomy Satellite. The β Pictoris disk is presented to Earth almost edge-on and is composed of solid particles in nearly coplanar orbits. The observed change in surface brightness with distance from the star implies that the mass density of the disk falls off with approximately the third power of the radius. Because the circumstellar material is in the form of a highly flattened disk rather than a spherical shell, it is presumed to be associated with planet formation. It seems likely that the system is relatively young and that planet formation either is occurring now around β Pictoris or has recently been completed.*

To the unaided eye, β Pictoris is a rather inconspicuous star in an equally obscure constellation and, located at far southerly declinations, it remains permanently below the horizon to much of Earth's Northern Hemisphere. At a distance of 16 parsecs (53 light-years), this fourth-magnitude star is considered a member, albeit somewhat remote, of the immediate solar neighborhood; it is classified as a main-sequence dwarf, similar to the sun in an evolutionary sense, but with twice the mass and probably ten times the luminosity (*1*). Interest in β Pictoris has increased greatly during the past year; observations by the Infrared Astronomy Satellite (IRAS) have led the IRAS investigator team to the conclusion that this star is surrounded by a cloud of cold, solid material, possibly in the form of a circumstellar disk (*2*). The IRAS investigators have also concluded that circumstellar material may be present around as many as one star in every five or ten and have suggested that, in the case of one of the stars (α Lyrae), the material may be associated with planet formation. Recently, we were successful in obtaining optical images of the disk, confirming its existence and tracing its extent from β Pictoris to more than twice the distance observed by IRAS.

Our observations were made at the Las Campanas Observatory (*3*) in Chile on 15 to 18 April 1984, using the du Pont 2.5-m telescope, a CCD camera (*4*), and a special optical instrument known as a coronagraph (*5*). The images of β Pictoris and those of a similar comparison star, α Pictoris, were taken through an optical filter centered at a wavelength of 890 nm, in the far-red region of the spectrum. The specially designed coronagraph was used to eliminate the starlight scattered into the immediate vicinity of the stellar image by diffraction from within the telescope, particularly that component of diffracted light created by the support structure for the telescope's secondary mirror. The coronagraph also contained a small (7 arcsec) circular mask positioned in the focal plane of the telescope to block out most of the light from the star. All data were digitized to an intensity range of 16 bits per pixel and recorded on magnetic tape.

The images obtained in Chile have been processed on both a Vicom image processing system at the University of Arizona and a similar DeAnza system at the Image Processing Laboratory of the Jet Propulsion Laboratory. After correcting for instrumental response and subtracting the contribution from the sky background, a series of ratio and difference images were created from normalized β and α Pictoris image pairs. Use of the α Pictoris images to correct for the scattered light around β Pictoris is made necessary by the relatively large difference between the brightness of the atmospherically scattered light from the star and the surface brightness of the disk itself. Even with the coronagraph, the scattered light from β Pictoris is three to five times brighter than the disk over most of the observable range. Were this not the case, the disk would surely have been discovered long ago by using conventional techniques with optical telescopes.

One example of the ratio images is shown in Fig. 1. The β Pictoris disk can be seen extending radially outward from the star, which was positioned behind the focal plane mask. The small spots appearing in Fig. 1 are positive (light) and negative (dark) images of faint field